Proceedings of the 21st ICSMGE, Vienna, Austria, 14 – 19 June 2026. Pistrol, Adam & Schweiger (eds.)
Published by: ÖGG, Austrian Society for Geomechanics, Salzburg, Austria, ISBN 978-3-9503898-4-5
https://doi.org/10.53243/ICSMGE2026-281

Innovative Framework for Railway Slope Performance Assessment in a Tropical Climate: Recent Advances.

Luiz Felipe Goulart Fiscina[1], Felipe Pacheco Silva[1], Felipe Santos de Almeida[1], Silvia Suzuki[1], Luciano de Oliveira[2], and Marcos Massao Futai[1].
Polytechnic School of the Universidade de São Paulo[1], São Paulo, Brazil, luizfiscina@usp.br
Vale S.A., Brazil[2]

ABSTRACT: Rainfall-induced landslides pose major challenges to the performance and safety of railway infrastructure in tropical regions. This study presents recent advances in the implementation of an integrated framework for assessing slope behavior along the Carajás Railway, Northeastern Amazon Biome - Brazil. The methodology, developed by the VALE in partnership with GeoInfraUSP, consists of eight stages; this paper focuses on preliminary results from stages (a) susceptibility mapping, (b) UAV-based inspection and mapping, (c) geological and hydro-geotechnical characterization, and (d) climate-informed numerical modeling. A 41-km pilot segment was selected due to its history of slope instabilities. Susceptibility mapping using InSAR and the Weight of Evidence method achieved an AUC of 86.9%, with strong correspondence to observed displacements. UAV-derived orthomosaics and LiDAR point clouds enabled detailed surface analysis and field validation. Hydro-geotechnical investigations revealed sandy, low-plasticity soils with high permeability across the Itapecuru Formation. Climate variability was analyzed using satellite datasets, such as CHIRPS for daily rainfall and SMAP for soil moisture, highlighting ENSO-related patterns. Transient seepage and stability analyses showed that slopes steeper than 40° approach failure conditions, especially under extreme rainfall. Lower safety factors were observed during La Niña years in the wet season (December–May), while El Niño years exhibited higher values in the dry season. Preliminary numerical thresholds linked to failure include daily rainfall ≥ 49 mm (P99) and 5-day totals ≥ 124 mm. The findings underscore the importance of integrating remote sensing, climate data, and field testing to anticipate geotechnical risks in data-scarce regions. Ongoing efforts include expanding the geological database, instrumenting critical slopes, and integrating machine learning, advanced numerical modeling, and bias-corrected CMIP6 climate projections. Future developments will incorporate heterogeneous slopes with benches and embankment sections, together with Material Point Method analyses for runout simulation and risk assessment, consolidating a comprehensive methodology for railway landslide management.

KEYWORDS: Railway Slopes Susceptibility Mapping, Remote Sensing, Hydro-Geotechnical Characterization, Numerical Analysis, Climate Variability.

1 INTRODUCTION

Landslides affecting linear infrastructure such as railways have increasingly posed operational, economic, and environmental challenges, especially in tropical regions where intense rainfall and complex geology converge (Palin et al., 2021; Sousa et al., 2025). In Brazil, the Carajás Railway (CR) is a critical logistic corridor that traverses geologically heterogeneous terrain, frequently affected by rainfall-induced slope instabilities (Sousa et al., 2025). Figure 1 illustrates representative slope instability features along the Carajás Railway.

Figure 1. Examples of slope instabilities observed along the Carajás Railway in Northeastern Amazon – Brazil (Futai et al., 2024).

Considering climate change projections and increasing rainfall extremes, improving slope risk assessment and long-term infrastructure resilience has become imperative. Conventional monitoring and inspection methods, while essential, face limitations in spatial coverage, temporal resolution, and early warning capability when applied to extensive and remote railway networks.

To address these challenges, the VALE Under Rail Research Chair, in partnership with the GeoInfraUSP Laboratory, proposed a multidisciplinary methodology to assess slope performance in tropical railway environments. This methodology was first presented by Futai et al. (2024) at the 7th Symposium on Railway Engineering in Brazil. It includes eight integrated stages, from remote susceptibility mapping to advanced numerical modeling and field experimentation (Figure 2). The goal is to develop a new approach for large-scale infrastructure risk analysis and detailed slope assessment.

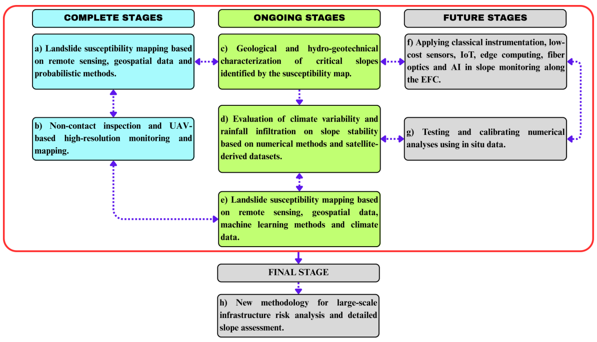

Figure 2. Integrated stages of the proposed methodology for slope performance assessment in tropical railway environments.

Building on that foundation, this paper presents the advances and partial results to date in the implementation of stages (a) to (d) of the proposed framework, namely: (a) landslide susceptibility mapping based on remote sensing, geospatial data and probabilistic methods; (b) non-contact inspection and UAV-based high-resolution monitoring and mapping; (c) geological and hydro-geotechnical characterization of critical slopes; and (d) preliminary evaluation of climate change and rainfall infiltration on slope stability based on numerical methods and satellite-derived datasets. The progress reported herein demonstrates the potential of emerging technologies to enhance the diagnosis, interpretation, and future risk modeling of geotechnical assets along the EFC.

2 LANDSLIDE SUSCEPTIBILITY MAPPING BASED ON REMOTE SENSING, GEOSPATIAL DATA AND PROBABILISTIC METHODS.

As part of the initial implementation of the proposed framework for assessing railway slope performance, a 41 km segment (km-370 to km-411) of the 900 km-long Carajás Railway (CR), located within the Pindaré River Watershed in northeastern Brazil, was selected as a pilot area (Figure 3). This region was chosen due to its high incidence of rainfall-induced landslides, documented instability events, and pronounced geomorphological variability (Sousa et al., 2025). The goal of this stage was to systematically evaluate landslide susceptibility by integrating terrain attributes, geological features, and land-use conditions derived from remote sensing data with probabilistic modeling techniques, aiming to produce a technically robust and spatially coherent susceptibility map encompassing natural slopes, anthropogenic cut slopes, and engineered embankments along the railway corridor.

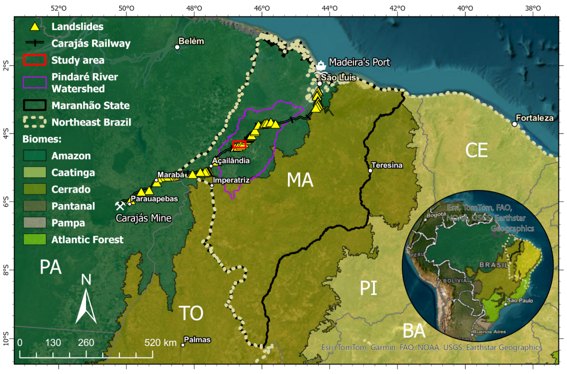

Figure 3. Location of the 41-km study segment (in red) of the Carajás Railway within the Pindaré River Watershed, Northeastern Amazon Biome - Brazil.

The analysis was conducted within a probabilistic framework employing the Weight of Evidence (WoE) method (Silva et al., 2025), implemented in a GIS environment to quantify the evidential weights of each conditioning factor based on the spatial relationship between mapped landslides and predictive variables. The model was subsequently validated using Interferometric Synthetic Aperture Radar (InSAR) data (Silva et al., 2025). Eleven conditioning factors were incorporated into the WoE analysis, including slope, elevation, curvature, Topographic Position Index (TPI), terrain roughness, lithology, soil type, land use/land cover, and proximity to faults and rivers. Continuous variables were discretized using the Natural Breaks (Jenks) classification, and the corresponding positive (W^+) and negative (W^-) evidential weights were combined to derive the Landslide Susceptibility Index (LSI).

According to Silva et al. (2025), the most influential factors included high terrain roughness (Wf = 3.73), proximity to geological faults (<1000 m, Wf = 3.67), steep slopes (>25°, Wf = 2.78), and areas close to rivers (<300 m), which exhibited the highest statistical weights.

The resulting Landslide Susceptibility Index (LSI) was validated through Receiver Operating Characteristic (ROC) analysis, yielding an Area Under the Curve (AUC) of 86.9% (Figure 4). Areas classified as very high susceptibility account for 14% of the study area and encompass 83.08% of the inventoried landslides (Figure 5). Ground displacement data derived from InSAR exhibited strong spatial correspondence with these high-risk zones, with subsidence rates reaching −47.3 mm/year and uplift up to 30.9 mm/year. Further methodological and analytical details can be found in Silva et al. (2025).

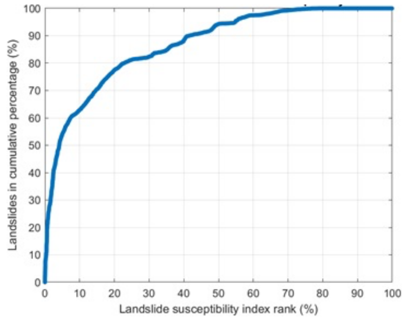

Figure 4 - Success rate curve of landslide susceptibility (Silva et al., 2025).

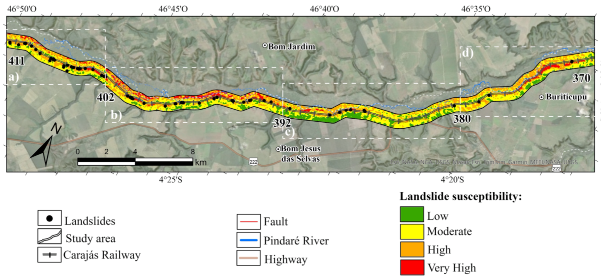

Figure 5. Landslide susceptibility map along the railway segment, generated using the Weight of Evidence (WoE) model. (a) km-411 to km-402; (b) km-402 to km-392; (c) km-392 to km-380; and (d) km-380 to km-370 (Silva et al., 2025).

Finally, these results underscore the effectiveness of integrating remote sensing and probabilistic modeling to assess slope instability and to support risk-informed decision-making in tropical infrastructure corridors.

3 NON-CONTACT INSPECTION AND UAV-BASED HIGH-RESOLUTION MONITORING AND MAPPING.

The integration of UAV-based surveys with susceptibility mapping was employed to verify and further characterize areas previously classified as highly prone to landslides. High-resolution orthomosaics and Digital Elevation Models (DEMs), generated through photogrammetry using RGB cameras and GNSS-RTK systems, enabled refined morphological analyses and the identification of instability-related surface features, in line with the methodologies and outcomes reported in prior studies such as those by Eker et al. (2017) and Ciccarese et al. (2024). Additionally, according to Silva et al. (2025), onboard LiDAR sensors allowed generating high-density 3D point clouds and detailed topographic models, which proved essential for the geometric characterization of slopes analyzed in detail at kilometer markers 374 along the CR (Figure 6). This integrated approach substantially enhanced the reliability of field validation for zones identified as highly susceptible by the predictive models.

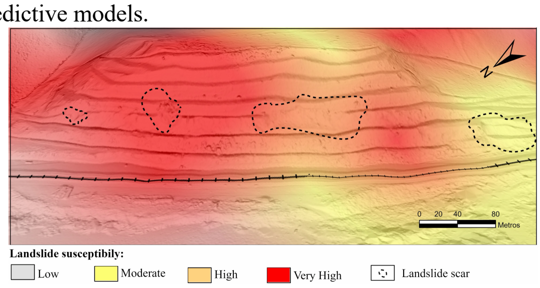

Figure 6. High-resolution topographic shaded reliefs of terraced slopes located near kilometer 374 along the Carajás Railway (CR).

4 GEOLOGICAL AND HYDRO-GEOTECHNICAL CHARACTERIZATION OF CRITICAL SLOPES.

The study area corresponds to the pilot sector defined within the integrated framework proposed by Silva et al. (2025), located between kilometers 370 and 411 of the Carajás Railway. This site was selected as a representative section to establish the methodological foundation for the subsequent stages of the research, including the geological and hydro-geotechnical characterization and the numerical analyses presented herein.

It is worth mentioning that this railway segment is situated within the geotectonic framework of the Parnaíba Basin, which originated during the Paleozoic Era. At that time, the deposition of the Serra Grande, Canindé, and Balsas groups occurred as part of the consolidation of the supercontinent Pangaea. Subsequent fragmentation of this landmass throughout the Mesozoic, along with the opening of the Atlantic Ocean, led to the accumulation of new sedimentary units, including the Mosquito, Pastos Bons, Corda, Grajaú, Codó, Itapecuru, and Ipixuna formations, as well as Cenozoic sediments (Lopes & Teixeira, 2013).

The Corda Formation (JKc), deposited in an arid environment, is composed of red to reddish-brown sandstones enriched with iron oxides and zeolites. This unit represents the basal sequence and is interdigitated with the Codó and Grajaú formations (Vaz et al., 2007). The Codó Formation (Kc), deposited under lacustrine conditions with marine incursions, consists of light gray sandstones, siltstones, evaporites, shales, and limestones. It is interdigitated with the Grajaú Formation and is overlain by the Itapecuru Formation (Paz & Rossetti, 2006). The Grajaú Formation (Kg), with deposits of fluvio-deltaic to eolian origin, comprises whitish to yellowish sandstones, claystone lenses, and quartz pebbles. Similarly to the Codó Formation, it is interdigitated with the Codó unit and overlain by the Itapecuru Formation (Klein & Sousa, 2012). The Itapecuru Formation (Kit), deposited under estuarine-lagoonal conditions, is composed of reddish grayish sandstones, siltstones, shales, and conglomerates. It conformably overlies the Codó and Grajaú formations, although local discontinuities may occur (Lima & Leite, 1978; Menezes et al., 2024).

Among the critical slopes analyzed in this study, the km-408 slope is highlighted. The primary geological units identified at this location are the Itapecuru, Grajaú/Codó, and Corda formations (Figure 7), indicating a geologically complex setting in which the railway infrastructure is embedded.

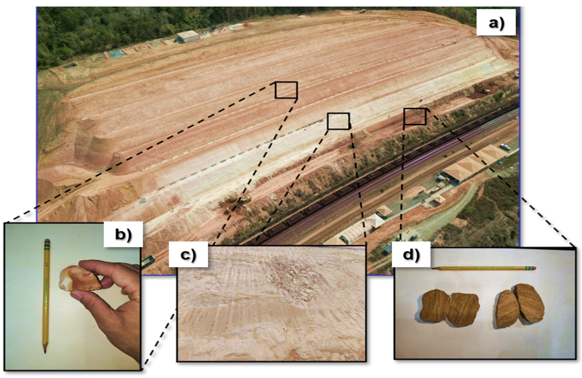

Figure 7. Different geological formations identified in the region. a) Slope km-408; b) Itapecuru Formation (Kit); c) Grajaú/Codó formation (Kg, Kc); d) Corda Formation (JKc).

Given the geological complexity and the regional climate marked by distinct wet and dry seasons, slope failures are mainly shallow landslides. These events may occur individually or evolve through surface erosion that weakens slope structures and can trigger larger mass movements. Such conditions emphasize the need to characterize the involved soils under saturated and unsaturated states, focusing on water flow behavior, as rainfall infiltration and suction loss are key triggering factors.

Field and laboratory investigations were therefore carried out, and the resulting soil profiles revealed marked heterogeneity, primarily attributed to weathering processes and environmental exposure. Grain-size distribution analyses indicated that the soils are predominantly sandy, with clay content varying both between and within formations. Samples from the Grajaú and Codó formations exhibited lower clay contents (approximately 4%), whereas the basal layers of the Itapecuru Formation displayed the highest concentrations, reaching up to 24%.

A key methodological advancement in this study was the use of automated and semi-automated equipment from METER, including the SATURO system for field infiltration and saturated permeability testing, and the HYPROP and WP4C devices for determining the Soil Water Characteristic Curve (SWCC). These tools enabled efficient and precise data acquisition, minimizing human error and reducing the need for manual intervention.

To support the geotechnical stability analysis, results from the initial series of laboratory and field tests on undisturbed soil blocks are presented. The samples were collected from areas within the Itapecuru Formation (near km-408), representing a lateritic profile typical of the Amazon region, as described by Costa (1991). Within the studied slopes, the Itapecuru Formation constitutes most of the stratigraphy, with thicknesses ranging from 25 to 40 meters. Table 1 summarizes typical geotechnical parameters obtained from these tests, as reported by Fiscina et al. (2025b). Furthermore, these parameters were derived from six undisturbed blocks collected within the Itapecuru Formation.

It is worth noting that the initial hydro-geotechnical characterization focused on materials from the Itapecuru Formation, given its predominance within the pilot segment and its relevance for numerical modeling. Ongoing tests are now being conducted on embankment materials and additional geological units along the railway, and their results will be presented in forthcoming publications.

Table 1 – Typical Geotechnical Properties of the Itapecuru Formation.

Parameter	Description	Average Value	Upper Value	Lower Value
W_{nat} (%)	Field moisture	7.1	12	3.8
γ_{nat}(kN/m³)	Natural density	18.8	19	16.7
γ_s (k N/m³)	Specific gravity	26.9	27	25.8
γ_d (kN/m³)	Dry density	17.6	17.8	16.1
γ_{sat}(kN/m³)	Saturated density	21	21.5	20
e	Void ratio	0.53	0.6	0.4
S_{nat} (%)	Natural Saturation degree	36	50	20
W_{sat} (%)	Saturated moisture	19.3	24	16
K_{sat} (m/s)	Field saturated permeability	4.2E-6	8.5E-6	1.17E-6
LL	Liquid limit	22	33	19
LP	Plasticity limit	15	25	13
IP	Plasticity index	7	8	4
SUCS	Soil unified classification		SC-SM	
c' (kPa)	Effective cohesion	0	0	0
Φ' (°)	Effective friction angle	36.5	37	34

The results indicate that the soil is predominantly sandy. Atterberg-limit tests revealed a low plasticity index, consistent with the presence of non-active clay minerals. Saturated triaxial tests confirmed mechanical behavior typical of sandy soils, characterized by negligible effective cohesion and an average internal friction angle of 36.5°. All triaxial tests yielded an effective cohesion (c') equal to 0 kPa, which is consistent with the frictional behavior of the Itapecuru Formation materials under the range of confining stresses applied in this study. A new series of triaxial tests will be performed under lower confining pressures (below 50 kPa) to verify the potential presence of small effective cohesion values associated with residual structure or cementation. One set of drained triaxial test conducted under natural-moisture conditions exhibited an apparent cohesion of 62.4 kPa, attributed to matric suction in the unsaturated state. These findings highlight the predominantly frictional response of the soil when fully saturated and the influence of suction under partially saturated conditions.

The Soil Water Characteristic Curve (SWCC) was fitted using data obtained from filter paper tests (FP), HYPROP-2, and WP4C devices. Figure 8 presents the resulting fit using the bimodal van Genuchten model (Seki et al., 2022), which adequately captured the distinct bimodal shape commonly observed in weathered tropical soils tropical soils, as reported by Fiscina et al. (2025b). The curve exhibited a low air-entry value ranging from 3 to 4 kPa. The wide range of saturation degrees observed in the field highlights the importance of an accurate SWCC representation, as in situ moisture conditions span a significant portion of the retention curve. The hydraulic conductivity function was estimated following the method proposed by Fredlund et al. (1994), using the saturated permeability (Ksat) as the starting point, as shown in Figure 9. Field permeability tests conducted with the SATURO device yielded a Ksat value of 4.20×10^{-6} m/s, further confirming the sandy nature of the soil. For additional details regarding the geotechnical parameters, see Fiscina et al. (2025b).

Finally, the data obtained from the tested sample were used as input for the transient slope stability analyses.

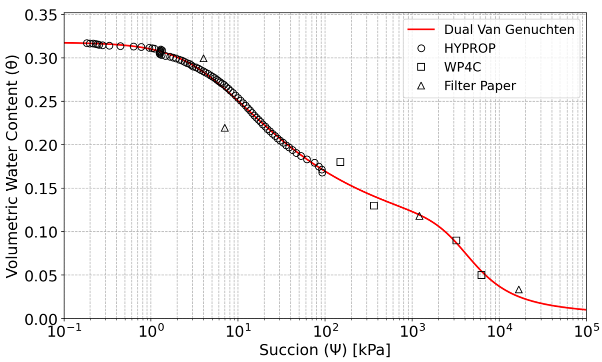

Figure 8. Soil Water Characteristic Curve of an Itapecuru Formation Sample.

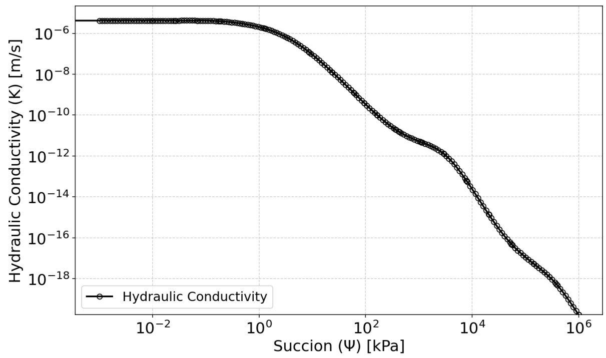

Figure 9. Permeability function of an Itapecuru Formation Sample.

5 PRELIMINARY EVALUATION OF CLIMATE VARIABILITY AND RAINFALL INFILTRATION ON SLOPE STABILITY BASED ON NUMERICAL METHODS AND SATELLITE-DERIVED DATASETS.

The Pindaré River Watershed (PRW), intersecting the critical km 370–411 segment of the Carajás Railway, experiences pronounced hydroclimatic variability and severe data scarcity, with only one rain gauge per 2,376 km² (Pereira Filho, 2018; Fiscina et al., 2025a). To address this limitation, five satellite-based precipitation datasets were evaluated, and CHIRPS was identified as the most accurate for climatological analyses over 1981–2023 (Fiscina et al., 2025a).

Fiscina et al. (2025a) identified three climatic zones within the watershed, each influenced by biome transitions, topography, and large-scale systems such as Intertropical Convergence Zone (ITCZ) and South Atlantic Convergence Zone (SACZ). Precipitation anomalies were strongly correlated with ENSO phases (La Niña increasing and El Niño reducing rainfall) with a consistent 3–5 month lag between ENSO signals and rainfall response. Trend analyses using the Mann-Kendall test and Sen's slope revealed no significant annual or seasonal changes, but a declining trend in August–September rainfall, which may heighten fire risk and soil desiccation before the wet season, affecting infiltration and slope stability timing.

To evaluate the implications of these climatic dynamics on slope behavior, a coupled numerical modeling study was conducted for typical cut slopes developed in the Itapecuru Formation, near km-408 (Fiscina et al., 2025b). Figure 10 illustrates the geomorphological features of this area. Using daily CHIRPS rainfall data from 2011 to 2023 (infiltration input) and SMAP-derived soil moisture data from 2016 to 2023 (used for suction calibration), transient seepage analyses were carried out in SEEP/W, followed by limit equilibrium slope stability analyses in SLOPE/W. The models simulated multiple slope inclinations (25°, 30°, 35°, and 40°) under different ENSO phases (El Niño, La Niña, and neutral years).

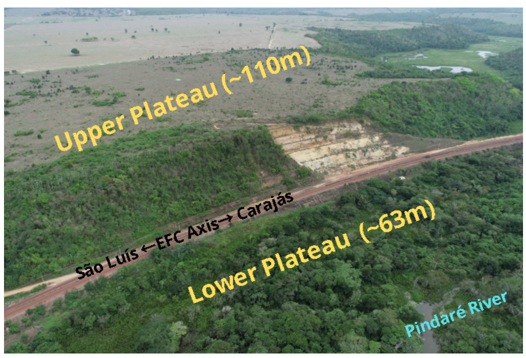

Figure 10. Representative geomorphological features of the slopes in the vicinity of the kilometer 408.

The models incorporated realistic boundary conditions reflecting seasonal variability, satellite-derived suction states, and field data. Transient infiltration simulated pore-pressure evolution, subsequently used in stability analyses. Unsaturated shear strength was represented by the Vanapalli et al. (1996) model, enabling the integration of suction effects into the limit-equilibrium framework and supporting a comprehensive evaluation of slope performance under climate-driven hydrological conditions. This approach enabled a comprehensive assessment of slope performance under climate-driven hydrological scenarios. Figure 11 summarizes the main characteristics of the numerical model.

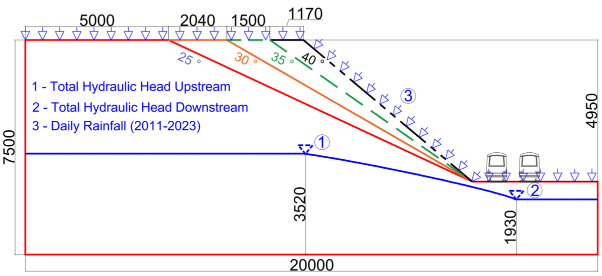

Figure 11. Main characteristics of the numerical model.

Results showed that 25° slopes remained stable (FS ≥ 1.5) throughout the rainfall series (Figure 12), while slopes steeper than 30° fell below safety thresholds of ABNT NBR 11682 (Fiscina et al., 2025b). Forty-degree slopes approached failure conditions (FS ≈ 1.0) under extreme rainfall (Figure 12). During La Niña years, safety factors decreased in the wet season (Dec–May), whereas El Niño years exhibited higher stability during the dry season, reflecting the non-linear response of slopes to seasonal and interannual rainfall variability.

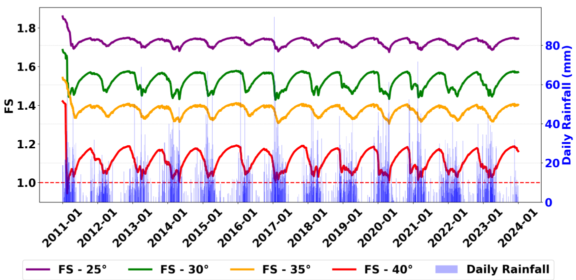

Figure 12. Variation of the Factor of Safety (FS) over the 2011–2023 time series for different slope angles.

Preliminary rainfall thresholds for instability were identified at daily precipitation above the 99th percentile (P99 ≥ 49 mm) and 5-day totals exceeding 124 mm (Fiscina et al., 2025b). These thresholds are particularly critical for slopes steeper than 35°, where transient infiltration reduces suction and sharply lowers safety factors. They may serve as initial references for slope monitoring protocols when combined with climate forecasts anticipating ENSO-related anomalies.

6 FUTURE STUDIES

Future developments of this research will focus on expanding the hydro-geotechnical characterization, refining numerical simulations, and improving susceptibility modeling to strengthen slope-risk assessment along the Carajás Railway. The current stage adopted homogeneous slope models without benches due to computational constraints and the long duration of transient analyses. Future studies will simulate more complex geometries, including bench configurations and variable material properties along the weathering profile, to better capture the influence of heterogeneity on infiltration and stability.

A complementary database containing the geometrical characteristics of past slope failures (depth, length, and relative position) is being integrated into the framework. This data will support future analyses using the Material Point Method (MPM), allowing the simulation of runout behavior and its potential impact on railway operations. This approach will also help distinguish the effects of short-duration, high-intensity rainfall from those of multi-day cumulative events, which may induce deeper or more extensive failures.

To broaden the representativeness of the analyses, new field and laboratory tests will be conducted in additional geological formations and embankment sections, enabling a more comprehensive understanding of hydro-mechanical responses across different materials and geometries. The resulting datasets will improve the calibration of numerical models and provide more realistic boundary and hydraulic conditions for slope-stability simulations. In addition, future simulations will incorporate climate-change scenarios derived from bias-corrected CMIP6 models available in the CLIMBRA database (Ballarin et al., 2023), allowing the assessment of long-term variations in rainfall intensity and frequency and their potential impacts on slope stability.

Machine-learning algorithms, such as Random Forest, will continue to be developed to integrate geomorphological, climatic, and geotechnical variables into data-driven susceptibility maps. In parallel, in-situ instrumentation will be deployed on selected slopes to monitor hydromechanical responses in real time and validate rainfall thresholds derived from modeling efforts.

It is worth emphasizing that the present work represents a partial phase of a broader framework. The current assumptions (homogeneous soils, plane-strain conditions, and focus on shallow failures triggered by suction loss) will be progressively refined as new data and modeling capabilities are incorporated. Ongoing developments aim to overcome these simplifications by including more complex slope geometries, heterogeneous materials, and post-failure analyses through MPM.

Ultimately, these forthcoming efforts will consolidate an integrated, adaptive, and data-driven methodology capable of coupling satellite-derived climatic information, laboratory and field data, and advanced numerical simulations. This will lead to a more reliable assessment of rainfall-induced landslide hazards and enhance the long-term resilience of railway infrastructure operating under tropical climatic conditions.

7 CONCLUSIONS

The integrated framework developed by GeoInfraUSP establishes a comprehensive methodology for assessing rainfall-induced slope instability in tropical railways. It integrates remote sensing, geomorphological analysis, hydro-geotechnical characterization, and climate-informed numerical modeling to support risk management and infrastructure resilience. This paper presents advances from the first implementation stages, focusing on the pilot area between kilometers 370 and 411 of the Carajás Railway.

The susceptibility analysis, based on a probabilistic Weight-of-Evidence (WoE) model integrated with InSAR data, showed strong predictive capacity (AUC = 86.9%). Very-high susceptibility zones cover 14% of the study area and contain 83% of mapped landslides, corresponding to InSAR ground displacements from −47.3 mm/year to +30.9 mm/year. The model incorporated conditioning factors representing both natural and engineered slopes broadening its applicability along the corridor.

The hydro-geotechnical characterization of the Itapecuru Formation clarified the mechanical and hydraulic behavior of lateritic soils typical of tropical environments. These materials display frictional behavior with low plasticity and apparent cohesion effects from suction under partially saturated conditions. Ongoing work extends this characterization to embankment materials and other geological units to enhance model calibration and regional representativeness.

Climatic analyses revealed the distinct influence of short-duration extremes and multi-day accumulations, helping define rainfall thresholds (P99 ≈ 49 mm/day; 5-day ≥ 124 mm) relevant for early warning. Numerical simulations so far used homogeneous slope models to evaluate long-term infiltration. Future developments will integrate bench geometries, heterogeneous materials, and failure databases with the Material Point Method (MPM) to simulate runout and operational impacts. Bias-corrected CMIP6 projections (CLIMBRA) will also assess future climate impacts. The integration of these techniques will yield a comprehensive methodology for rainfall-induced landslide risk assessment along the entire Carajás Railway.

These advances represent a coherent step in implementing the framework, confirming its technical robustness and adaptability. The integration of probabilistic, geotechnical, and climatic components forms a solid foundation for improving slope-risk assessment and enhancing the resilience of railway infrastructure in tropical environments.

8 ACKNOWLEDGEMENTS

This work was supported by the Cátedra Under Rail. The authors also acknowledge financial support from CAPES and the research productivity fellowship from CNPq (grant 401105/2025-3).

9 REFERENCES

Associação Brasileira de Normas Técnicas (ABNT). (2009). NBR 11682: Estabilidade de encostas [Slope stability]. ABNT, Rio de Janeiro.

Ballarin, A. S., Sone, J. S., Gesualdo, G. C., Schwamback, D., Reis, A., Almagro, A., & Wendland, E. C. (2023). CLIMBra—climate change dataset for Brazil. Scientific Data, 10(1), 47. https://doi.org/10.1038/s41597-023-01988-8

Ciccarese, G., Tondo, M., Mulas, M., Bertolini, G., & Corsini, A. (2024). Rapid assessment of landslide dynamics by UAV-RTK repeated surveys using ground targets: The Ca' Lita Landslide (Northern Apennines, Italy). Remote Sensing, 16(6), 1032. https://doi.org/10.3390/rs16061032

Costa, M. L. (1991). Aspectos geológicos dos lateritos da Amazônia. Brazilian Journal of Geology, 21(2), 146–160.

Eker, R., Aydın, A., & Hübl, J. (2017). Unmanned aerial vehicle (UAV)-based monitoring of a landslide: Gallenzerkogel landslide (Ybbs-Lower Austria) case study. Environmental Monitoring and Assessment, 190(1). https://doi.org/10.1007/s10661-017-6402-8

Fiscina, L. F. G., Silva, M. E. S., Silva, F. P., Vitteli, G., & Futai, M. M. (2025a). Satellite-derived precipitation trends and ENSO-related anomalies in the Pindaré River Watershed, Northeastern Amazon Biome. Earth Systems and Environment (in press). DOI: 10.1007/s41748-025-00743-7

Fiscina, L.F.G., Almeida, F.S., Futai, M.M. (2025b). Numerical Simulation of Infiltration in Cut Slopes of the Itapecuru Formation During ENSO Years Based on Satellite Data: A Climatic Study in the Northeastern Amazon Region, Brazil. In IX Brazilian Conference on Slope Stability (COBRAE), Bento Gonçalves, Brazil (accepted).

Fredlund, D. G., Xing, A., & Huang, S. (1994). Predicting the permeability function for unsaturated soils using the soil-water characteristic curve. Canadian Geotechnical Journal, 31(4), 533–546.

Futai, M. M., Oliveira, L., Goulart Fiscina, L. F., Quevedo, R. P., Sousa, M. T. R., Araújo, G. R. M. B., Poncetti, B. L., Assis, L. S., Silveira, R. M., Andrade, J. A., Monticelli, J. P., Suzuki, S., & Silva, T. B. (2024). Application of new technologies for the evaluation of railway slope performance in a tropical region. In VII Symposium on Railway Engineering, Campinas, Brazil, May 13–14, 2024.

Klein, E. L., & Sousa, C. S. D. (2012). Geology and mineral resources of the state of Maranhão. CPRM.

Lima, E. D. A. M., & Leite, J. F. (1978). Global study project of the mineral resources of the Parnaíba sedimentary basin: Geological–metallogenetic integration. CPRM.

Lopes, E. C. dos S., & Teixeira, S. G. (2013). Geological context. In I. C. N. Bandeira (Ed.), Geodiversity of the state of Maranhão (p. 15). CPRM.

Menezes, M. N., Dal'Bó, P. F., Smith, J. J., Borghi, L., Arena, M., Favoreto, J., & de Araújo-Júnior, H. I. (2024). Pedogenic processes and climatic conditions from Cretaceous (Albian) tropical paleosols of the Itapecuru Formation, Parnaíba Basin, northeast Brazil. Palaeogeography, Palaeoclimatology, Palaeoecology, 633, 111881.

Palin, E. J., Scaife, A. A., Arribas, A., Dunstone, N., & Bett, P. E. (2021). Implications of climate change for railway infrastructure. Wiley Interdisciplinary Reviews: Climate Change, 12(5), e728.

Paz, J. D., & Rossetti, D. F. (2006). Petrography of gypsum-bearing facies of the Codó Formation (Late Aptian), northern Brazil. Annals of the Brazilian Academy of Sciences, 78, 557–572.

Pereira Filho, A. J., Vernado, F., Vernado, G., Gomes Vieira Reis, F. A., Giordano, L. D. C., Cerri, R. I., Santos, C. C. D., Sampaio Lopes, E. S., Gramani, M. F., Ogura, A. T., Zaine, J. E., Cerri, L. E. D. S., Augusto Filho, O., D'Affonseca, F. M., & Amaral, C. D. S. (2018). A step towards integrating CMORPH precipitation estimation with rain gauge measurements. Advances in Meteorology, 2018, 1–24. https://doi.org/10.1155/2018/2095304

Seki, K., Toride, N., & van Genuchten, M. Th. (2022). Closed-form hydraulic conductivity equations for multimodal unsaturated soil hydraulic properties. Vadose Zone Journal, 21(1), e20168.

Silva, F.P., Fiscina, L.F.G., de Almeida, F.S. et al. Landslide Susceptibility Modeling in a Railway in the Amazon Region: Integration of the Weight of Evidence (WOE) Method and InSAR Monitoring Data. Geotech Geol Eng 43, 438 (2025). https://doi.org/10.1007/s10706-025-03418-2

Sousa, M. T. R., Silva, F. P., Fiscina, L. F. G., Cordeiro, W. B., & Futai, M. M. (2025). Analysis of land use and coverage and its relationships with slope instability events on the Carajás Railway: The case of the Pindaré River Basin in the Brazilian Amazon biome. Journal of South American Earth Sciences, 145, 105373. https://doi.org/10.1016/j.jsames.2025.105373

Vanapalli, S. K., Fredlund, D. G., Pufahl, D. E., & Clifton, A. W. (1996). Model for the prediction of shear strength with respect to soil suction. Canadian Geotechnical Journal, 33(3), 379–392.

Vaz, P. T., Wanderley Filho, J. R., & Travassos, W. A. S. (2007). Parnaíba Basin. Petrobras Geoscience Bulletin, 15(2), 253–263.